A novel approach to the synthesis of photoluminescent germanium nanoparticles by reactive laser ablation

View the table of contents for this issue, or go to the journal homepage for more

A novel approach to the synthesis of photoluminescent germanium nanoparticles by reactive laser ablation

Daria Riabinina[1]**, Christophe Durand**[1]**, Mohamed Chaker**[1]**, Nelson Rowell**[2] **and Federico Rosei**[1]

[1] INRS-EMT, Université du Québec, 1650 Lionel-Boulet, C.P. 1020, Varennes (Qc), J3X 1S2, Canada
[2] National Research Council, Institute for National Measurement Standards, Ottawa, ON, K1A 0R6, Canada

E-mail: riabinina@emt.inrs.ca and chaker@emt.inrs.ca

Abstract
We propose a novel approach to the synthesis of photoluminescent Ge nanoparticles using reactive laser ablation. The deposition of germanium under low oxygen pressure (2–100 mTorr) yields Ge nanoparticles embedded in a Ge oxide matrix. Ge nanostructures were characterized by transmission electron microscopy, x-ray photoelectron spectroscopy and photoluminescence (PL) spectroscopy. The oxygen pressure determines the degree of oxidation of GeO_x films ($0 \leqslant x \leqslant 2$). A strong PL signal depending on oxygen pressure was observed. The PL maximum is detected for 10 mTorr of oxygen corresponding to a nanoparticle size of 1.8 ± 0.5 nm.

1. Introduction

The quantum confinement effect in group IV semiconductors has recently attracted considerable interest due to possible applications in optoelectronic devices. Quantum confinement paves the way to obtaining good luminescent properties for semiconductors with an indirect bandgap. Following Canham's report of intense visible photoluminescence from porous silicon [1], and the work of Maeda *et al* on Ge microcrystals [2], much experimental and theoretical work has been published on Si and Ge nanostructures. For instance, Galli and co-workers have studied the structure and stability of Ge nanoparticles [3], and also the effects of surface reconstruction [4]. Si and Ge nanostructures were synthesized in many ways, including etching, implantation, co-sputtering, sol–gel, laser ablation etc [5–12]. At present the most common method of fabrication of luminescent Ge structures is the synthesis of Ge nanocrystals embedded in a SiO_2 matrix by implantation or sputtering [13–15]. Although significant photoluminescence properties have been reported, the non-uniform size distribution, the low density of nanoparticles, the weak photoluminescence efficiency and the limited size control remain critical issues.

Herein we propose a novel one-step synthesis method for Ge nanoparticles embedded in a GeO_2 matrix: reactive pulsed laser deposition (R-PLD), i.e. PLD under a background pressure of a reactive gas. PLD is a versatile technique for the synthesis of nanostructured materials. For example, PLD of silicon under an inert gas pressure allows the synthesis of photoluminescent nanoparticles with a controlled size [5, 16–18]. However, Ge nanoparticles synthesized by PLD in an inert gas atmosphere do not exhibit significant luminescent properties. Such nanostructures may be rendered luminescent by post-deposition processing (e.g. rapid thermal annealing or oxidation) [19]. The advantage of R-PLD under oxygen pressure is the extremely simple one-step synthesis of both Ge nanoparticles and a GeO_2 matrix. In this paper we describe the synthesis of amorphous Ge nanoparticles that are highly photoluminescent without any post-annealing treatment.

2. Experimental details

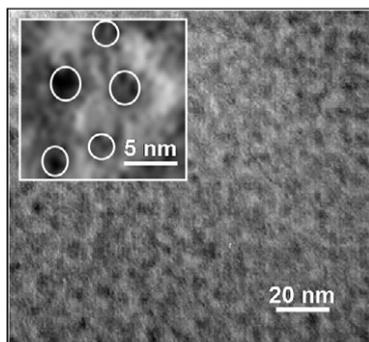Germanium oxide (GeO_x, $0 \leqslant x \leqslant 2$) films were deposited by conventional PLD under a low oxygen background pressure

Figure 1. TEM image of GeO$_x$ film deposited under 10 mTorr of oxygen.
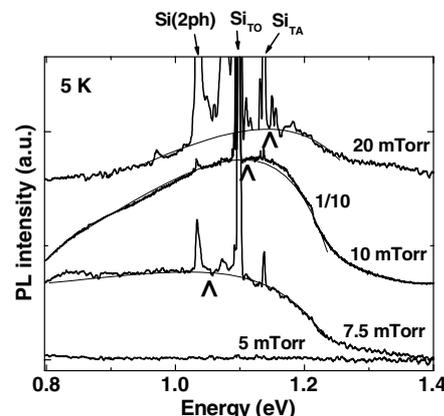

Figure 2. Photoluminescence spectra at 5 K as a function of oxygen pressure. The PL spectra were adjusted for better comparison and the scaling factor is shown in the figure. The symbol ∧ indicates the maximum of the PL spectra. The peaks at 1.034, 1.099 and 1.138 eV are related to two-phonon, TO (transverse-optical) and TA (transverse-acoustic) phonon-assisted transitions in the Si substrate.

(2–50 mTorr) on Si substrates[3]. A rotating Ge target (purity 99.99%) was ablated by an excimer KrF laser ($\lambda = 248$ nm) with pulse duration 17 ns and repetition rate 20 Hz. The laser density and substrate–target distance were fixed at 5 J cm^{-2} and 40 mm, respectively.

The optical and structural properties of deposited films were studied by photoluminescence spectroscopy (PL), transmission electron microscopy (TEM) and x-ray photoelectron spectroscopy (XPS). The PL spectra of the samples were measured at low temperature (5 K) using the 458 nm line of an Ar$^+$ laser (46 mW). Conventional transmission electron microscopy (TEM) observations were made using a JEOL 200CX operated at an accelerating voltage of 200 kV. Deposition of ultra-thin films (∼50 nm) was carried out on Cu/C TEM grids to observe the film microstructure. For XPS analysis, the sample surface was sputtered for short durations by an Ar ion beam at 5 keV for 1 min (etch rate ∼20 Å min^{-1}) to remove the native oxide and the organic surface contamination. Due to the insulating properties of Ge oxide, a slight charge shift of the XPS spectra was observed for the films deposited under high oxygen pressure. This effect was systematically corrected by positioning the Ge 3d core level peak from the non-oxidized germanium at 29.3 eV, when this peak was detected. When this peak could not be used, the shift was corrected by positioning the Ge 3d peak from GeO$_2$ at 32.7 eV. This procedure is accurate enough to fit the Ge 3d with five contributions at fixed energies (error less than ±0.1 eV).

3. Results

Figure 1 displays a TEM image of a 20 nm-thick GeO$_x$ film deposited on a TEM grid under 10 mTorr of oxygen. We observe a granular structure that can be attributed to the presence of nanoparticles. The average size of the nanoparticles was found to be equal to about 2–3 nm in diameter, as shown in the inset of figure 1.

Figure 2 shows low temperature PL spectra of Ge deposited by PLD under various oxygen pressures (between 5 and 20 mTorr). A remarkable increase in PL intensity (by a factor of 20) was observed at 10 mTorr. The maximum of the PL spectra shifts from 1.05 to 1.18 eV by increasing the oxygen pressure from 7.5 to 20 mTorr.

---

[3] The thickness of the deposited films was ∼200 nm, as measured by imaging the sample section by scanning electron microscopy.

Table 1. Nanoparticle size d^{PL} and d_{adj}^{XPS} calculated from PL and XPS data, respectively. C_{Ge}^{XPS}, concentration of Ge^0 obtained from XPS spectra; f_{Ge}, volume fraction of Ge^0; d_{adj}^{XPS}, Ge nanoparticle size calculated using XPS data (without a Ge-suboxide shell).

P (mTorr)	d^{PL} (nm)	C_{Ge}^{XPS} (%)	f_{Ge} (%)	d_{adj}^{XPS} (nm)
20	**1.7** (±0.3)	0.5 (±0.1)	0.3 (±0.05)	**1.6** (±0.5)
10	**1.9** (±0.3)	0.7 (±0.1)	0.4 (±0.05)	**1.7** (±0.5)
7.5	>**2.3** (±0.6)	21.4 (±0.1)	13.2 (±0.05)	**9.1** (±0.5)

The origin of the observed photoluminescence can be explained by different factors. Firstly, the observed PL spectra can originate from the presence of Ge nanoparticles. The PL in the infra-red region was experimentally observed by Takeoka et al for Ge nanocrystals embedded in Si oxide [13]. An empirical and theoretical correlation between the position of the PL spectral maximum and nanoparticle size was established. The divergence between experimental results and the theoretical model proposed by Niquet et al was described in terms of carrier trapping on surface defects [20]. Secondly, the origin of the PL spectra of the Ge oxide system can be due to oxide defects. It was also previously shown that Ge oxide and Si oxide systems emit in the blue–green region from 2 to 2.5 eV [14, 20]. As this recombination energy is much higher than the bandgap value of Ge and is size independent, this photoluminescence is attributed to oxide defects.

In light of that discussion, we expect that the PL observed for GeO$_x$ samples is due to the presence of Ge nanoparticles. The PL peak shift is attributed to the variation of nanoparticle size as a function of oxygen pressure. Using the established correlation (based on carrier confinement effects) between Ge nanoparticle size and the position of PL spectra [13], we estimated the size of Ge nanoparticles d^{PL} to be 1.9 ± 0.3 nm and 1.7 ± 0.3 nm for the samples deposited under 10 and 20 mTorr, respectively (table 1). This value is in good agreement with the nanoparticle size observed by TEM. For 7.5 mTorr, we observe a quasi-constant luminescence from 1.05 to 0.8 eV that we attribute to the wide nanoparticle size distribution with the lower limit of 2.3 nm. As in [10], we
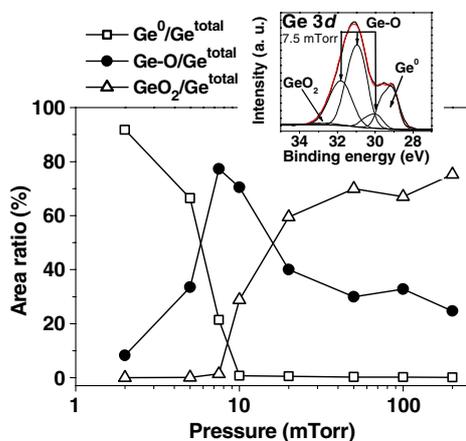
Figure 3. The evolution of ratios Ge^0/Ge^{total}, Ge–O/Ge^{total} and GeO$_2$/Ge^{total} as a function of oxygen pressure. The inset shows the fit of the Ge 3d signal at 7.5 mTorr by five peaks corresponding to Ge (Ge^0), Ge–O (Ge^{1+}, Ge^{2+}, Ge^{3+}) and GeO$_2$ (Ge^{4+}) contributions.

(This figure is in colour only in the electronic version)

observed a drastic increase of PL intensity for a nanoparticle size of ~2 nm. A further decrease of PL intensity at 20 mTorr of O$_2$ could be explained by a low density and low size of Ge nanoparticles or by the low absorbance of the light used for excitation.

Takeoka *et al* also proposed a correlation between nanoparticle size and volume fraction of Ge [13]. Assuming a uniform distribution of nanoparticles, the spherical Ge nanoparticles are arranged in a simple cubic lattice with a lattice constant $(s + d_{ave})$ and cell volume $(s + d_{ave})^3$, where d_{ave} is the average nanoparticle size with volume $(4\pi/3)(d_{ave}/2)^3$ and s is the inter-nanoparticle distance. The relationship between the Ge volume fraction f_{Ge} (%) and nanoparticle size d_{ave} is thus expressed as:

$$\frac{f_{Ge}}{100} = \frac{(4/3)\pi(d_{ave}/2)^3}{(s + d_{ave})^3} \qquad (1)$$

where s is empirically found to be 5 nm for the Ge/SiO$_2$ system [13]. As this model is independent of the surrounding material, we can apply it to a variety of systems including the Ge/GeO$_2$ system. Therefore, XPS measurements were performed to estimate the volume fraction of Ge and evaluate the nanoparticle size (d_{ave}^{XPS}).

The evolution of the Ge 3d XPS peak with increasing O$_2$ pressure clearly shows a progressive oxidation of germanium. The Ge 3d signals were fitted using five contributions corresponding to the non-oxidized Ge^0 and Ge^{1+}, Ge^{2+}, Ge^{3+} and Ge^{4+} oxidation states, as shown for a pressure of 7.5 mTorr in the inset of figure 3 (Ge^{4+} is associated with GeO$_2$). The relative positions of all Ge contributions were taken from the literature [21] (chemical shift of 0.85 eV per oxidation state) and were fixed for all oxygen pressures. We plot in figure 3 the area ratios Ge^0/Ge^{total}, Ge–O/Ge^{total} and GeO$_2$/Ge^{total} (where Ge^0 is non-oxidized Ge, GeO$_2$ is Ge dioxide, Ge^{total} is the total Ge 3d area and Ge–O is the sum of Ge sub-oxide peak areas, i.e. Ge^{1+}, Ge^{2+}, Ge^{3+}).

This analysis shows that the components of the Ge 3d signals exhibit a transition region between 7.5 and 20 mTorr.

Below 5 mTorr, the sample is mainly composed of non-oxidized Ge. At 7.5 mTorr, most Ge atoms (~77%) are involved in sub-oxide compounds (GeO$_{x<2}$) to the detriment of non-oxidized Ge (~21%). At rather higher pressures of O$_2$, the composition is about 75% GeO$_2$ and 25% Ge–O. This XPS analysis clearly demonstrates a high control of Ge oxidation by R-PLD.

The optimal condition for the formation of photoluminescent Ge nanoparticles embedded in a GeO$_{x<2}$ matrix appears to be 10 mTorr of oxygen. At this pressure, the relative concentration of non-oxidized germanium $C_{Ge}^{XPS} = $ Ge^0/Ge^{total} is extremely low (0.7%). At low pressure, the nanoparticles are presumably too large (several nanometres in diameter) for effective PL. At 20 mTorr, since C_{Ge}^{XPS} decreases down to 0.5%, we expect a decrease in nanoparticle size. Beyond 20 mTorr, the C_{Ge}^{XPS} is below 0.2%, which corresponds to the XPS detection limit. The relation between the C_{Ge}^{XPS} obtained by XPS and the volume fraction f_{Ge} can be expressed by:

$$f_{Ge} = \frac{C_{Ge}^{XPS}/\rho_{Ge}}{C_{Ge}^{XPS}/\rho_{Ge} + (1 - C_{Ge}^{XPS})/\rho_{GeO_2}} \qquad (2)$$

where ρ_{Ge} and ρ_{GeO_2} are the Ge and GeO$_2$ volume densities[4]. Using equation (1), we estimated the size of the Ge core of nanoparticles d_{ave}^{XPS} (table 1).

Since d_{ave}^{XPS} is calculated using C_{Ge}^{XPS} (taking into account only Ge–Ge bonds), this value describes only the Ge nanoparticle core. As the nanoparticle is surrounded by the Ge-suboxide shell, we adjust the size of the nanoparticles as follows: $d_{adj}^{XPS} = d_{ave}^{XPS} + 2l$ with $2l = 0.5$ nm, where l is the estimated shell thickness (table 1)[5] [22].

At 10 and 20 mTorr, the nanoparticle size d^{PL} is in good agreement with d_{adj}^{XPS}, and these results are confirmed by TEM images for 10 mTorr samples (figure 1). At 7.5 mTorr, nanoparticle sizes estimated from PL and XPS data are different. As the PL spectrum suggests a wide size distribution, the average size d_{adj}^{XPS} obtained from XPS is not representative. Therefore, at 7.5 mTorr, the actual size of photoluminescent nanoparticles is that obtained from PL data ($d^{PL} \geqslant 2.3 \pm 0.6$ nm).

4. Conclusion

In conclusion, a simple approach based on reactive PLD (without annealing treatment) was used to synthesize photoluminescent Ge nanoparticles. The degree of effective Ge oxidation can be directly controlled by varying the oxygen background pressure during the ablation process. The concentration of non-oxidized Ge determines the nanoparticle size, and hence the PL properties. The maximum PL intensity is observed for the sample deposited under an oxygen pressure of 10 mTorr corresponding to a nanoparticle size of ~1.8 ± 0.5 nm.

[4] The volume densities ρ_{Ge} and ρ_{GeO_2} were calculated using $\rho = Z/v$, where Z is the number of formulae in the unit cell and v is the volume of the elementary unit cell.
[5] To calculate the adjusted nanoparticle size, we estimated the shell thickness as $l = \frac{1}{2}(l_{Ge-Ge} + l_{Ge-O}) = 2.45$ Å, where the Ge–Ge bond length l_{Ge-Ge} is equal to 3.2 Å in amorphous Ge and the Ge–O bond length l_{Ge-O} is equal to 1.73 Å in amorphous GeO$_2$.

Acknowledgments

References

[1] Canham L 1990 *Appl. Phys. Lett.* **57** 1046
[2] Maeda Y, Tsukamoto N, Yazawa Y, Kanemitsu Y and Masumoto Y 1991 *Appl. Phys. Lett.* **59** 3168
[3] Pizzagali L, Galli G, Klepeis J E and Gygi F 2001 *Phys. Rev. B* **63** 165324
[4] Puzder A, Williamson A J, Roberedo F A and Galli G 2003 *Phys. Rev. Lett.* **91** 157405
[5] Kabashin A V, Sylvestre J P, Patskovsky S and Meunier M 2002 *J. Appl. Phys.* **91** 3248
[6] Franzo G, Iacona F, Spinella C, Cammarata S and Grimbaldi M G 2000 *Mater. Sci. Eng. B* **69** 454
[7] Smirani R, Martin F, Abel G, Wang Y Q and Ross G G 2005 *Nanotechnology* **16** 32
[8] Mimura A, Fujii M, Hayashi S, Kovalev D and Koch F 2000 *Phys. Rev. B* **62** 12625
[9] Takeoka S, Toshikiyo K, Fujii M, Hayashi S and Yamamoto K 2000 *Phys. Rev. B* **61** 15988
[10] Kolobov A V, Wei S Q, Yan W S, Oyanagi H, Maeda Y and Tanaka K 2003 *Phys. Rev. B* **67** 195314
[11] Yang H Q, Wang X J, Shi H Z, Xie S, Wang F, Gu X and Yao X 2002 *Appl. Phys. Lett.* **81** 5144
[12] Jie Y X, Wee A T S, Huan C H A, Sun W X, Shen Z H and Chua S J 2004 *Mater. Sci. Eng. B* **107** 25
[13] Takeoka S, Fujii M, Hayashi S and Yamamoto K 1998 *Phys. Rev. B* **58** 7921
[14] Maeda Y 1995 *Phys. Rev. B* **51** 1658
[15] Saito A and Suemoto T 1997 *Phys. Rev. B* **56** R1688
[16] Dolbec R, Irissou E, Chaker M, Guay D, Rosei F and El Khakani M A 2004 *Phys. Rev. B* **70** 201406
[17] Patrone L, Nelson D, Safarov V I, Sentis M and Marine W 2000 *J. Appl. Phys.* **87** 3829
[18] Seto T, Orii T, Hirasawa M and Aya N 2003 *Thin Solid Films* **437** 230
[19] Ma X, Yan Z, Yuan B and Li B 2005 *Nanotechnology* **16** 832
[20] Niquet Y M, Allan G, Delerue C and Lannoo M 2000 *Appl. Phys. Lett.* **77** 1182
[21] Schmeisser D, Schnell R D, Bogen A, Himpsel F J, Rieger D, Landgren G and Morar J F 1986 *Surf. Sci.* **172** 455
[22] Gutierrez G and Rogan J 2004 *Phys. Rev. E* **69** 031201